A New Type of Isolator for Millimeter-Wave Integrated Circuits Using a Nonreciprocal Traveling-Wave Resonator

MASAHIRO MURAGUCHI, STUDENT MEMBER, IEEE, KIYOMICHI ARAKI, AND YOSHIYUKI NAITO, SENIOR MEMBER, IEEE

Abstract —**A nonreciprocal traveling-wave resonator critically coupled to a waveguide becomes an isolator with high isolation. The dielectric image-line isolator with a magnetized ferrite pillbox as the nonreciprocal traveling-wave resonator is described. The validity of the theory is verified by experiments carried out at the 50-GHz range. The theoretical and experimental estimations of the coupling coefficient between a pillbox resonator and a straight dielectric waveguide are also included.**

I. Introduction

DIELECTRIC open waveguides are emerging as an important vehicle for realizing integrated circuits in the region from millimeter-wave to optical-wave. Many passive and active millimeter-wave devices have been developed with dielectric open waveguides such as dielectric image lines [1]. Nonreciprocal devices, e.g., circulators and isolators, are highly useful building components in the millimeter-wave integrated circuits. Several efforts have been made to realize such devices on the dielectric open waveguide—for example, the dielectric image lines [1]–[3], the rectangular dielectric waveguides [3], and the dielectric slab waveguides [4], [5]; their experimental results are not sufficient, however. The difficulties on these structures are caused by the radiation from the curved surface of the device and reduced nonreciprocity owing mainly to the weak energy confinement in ferrite.

This paper proposes a new configuration of isolator. The device consists of a directional coupler and a nonreciprocal phase shifter as shown in Fig. 1. The closed-loop structure including the nonreciprocal phase shifter becomes a nonreciprocal traveling-wave resonator because a traveling-wave arises in the loop. In this circuit, the wave transmission from port 2 to port 1 can be eliminated by properly adjusting the coupling coefficient of the directional coupler, while the wave transmission from port 1 to port 2 is scarcely affected by the resonator at the same frequency. Under this situation, all of the transmission power from port 2 to port 1 is dissipated in the resonator by its losses without any reflected power.

Manuscript received April 2, 1982; revised June 2, 1982. This work was supported in part by Scientific Research Grant-In-Aid from the Ministry of Education of Japan, under Grant 56460108.

The authors are with the Department of Electrical and Electronic Engineering, Tokyo Institute of Technology, 2-12-1, O-okayama, Meguro-ku, Tokyo 152, Japan.

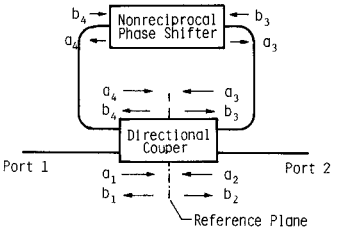

Fig. 1. Schematic of an isolator using a nonreciprocal traveling-wave resonator.

The nonreciprocal traveling-wave resonator is actually realized by a magnetized ferrite pillbox resonator distributionally coupled to a dielectric waveguide. The millimeter-wave isolator using the ferrite pillbox resonator has a number of attractive features: 1) the structure is very simple; 2) the isolation is very high; 3) the insertion loss is low; and 4) the operation frequency can easily be swept by changing the applied magnetic field. The validity of the theory is verified by experiments carried out at the 50-GHz range.

The theoretical and experimental estimations of coupling coefficient between a pillbox resonator and a straight dielectric waveguide are also described.

II. Basic Considerations of the Isolator Using a Traveling-Wave Resonator

Consider a traveling-wave resonator circuit as shown in Fig. 1. The phase shifter can be realized by a waveguide of proper length and the closed-loop structure consisting of its waveguide becomes a resonator. When the waveguides are image lines, microstrip lines, or metal rectangular waveguides, the circuits are called traveling-wave ring circuits. They were used as waveguide traveling-wave power multipliers [6], [7], where the phase shifters were reciprocal. A nonreciprocal ring circuit was initially studied by Tischer for the purpose of measuring the material constants of ferrite [8]. However, it is not known that such a ring circuit has a critical coupling condition just as in the case of a one-port cavity resonator circuit.[1]

Let a_i and b_i, respectively, be the incident and reflected

[1]E.-G. Neumann *et al.*, mentioned a critical coupling for a reciprocal ring resonator to measure its radiation loss in [9].

0018-9480/82/1100-1867$00.75 ©1982 IEEE

normalized wave amplitudes at the reference plane, where i indicates the port number of the directional coupler. The scattering-matrix equations of the directional coupler and nonreciprocal phase shifter can, respectively, be expressed as follows:

$$\begin{bmatrix} b_1 \\ b_2 \\ b_3 \\ b_4 \end{bmatrix} = \begin{bmatrix} 0 & S_{12} & S_{13} & 0 \\ S_{21} & 0 & 0 & S_{24} \\ S_{31} & 0 & 0 & S_{34} \\ 0 & S_{42} & S_{43} & 0 \end{bmatrix} \begin{bmatrix} a_1 \\ a_2 \\ a_3 \\ a_4 \end{bmatrix} \tag{1}$$

and

$$\begin{bmatrix} a_4 \\ a_3 \end{bmatrix} = \begin{bmatrix} e^{-\phi_f} & 0 \\ 0 & e^{-\phi_b} \end{bmatrix} \begin{bmatrix} b_3 \\ b_4 \end{bmatrix}. \tag{2}$$

When port 2 is terminated with a matched load and the circuit is fed at port 1, the following relation is obtained:

$$\frac{b_2}{a_1} = \frac{S_{21} - (S_{21}S_{34} - S_{24}S_{31})e^{-\phi_f}}{1 - S_{34}e^{-\phi_f}} \tag{3}$$

where $a_2 = a_3 = 0$. It can easily be shown that, if the directional coupler is perfect, there is no reflection for any coupling conditions. Here we call $|b_2/a_1|^2$ the forward transmission coefficient.

Similarly, when the port 1 is terminated with a matched load and the circuit is fed at the port 2, the following relation is obtained:

$$\frac{b_1}{a_2} = \frac{S_{12} - (S_{12}S_{43} - S_{13}S_{42})e^{-\phi_b}}{1 - S_{43}e^{-\phi_b}} \tag{4}$$

where $a_1 = a_4 = 0$. We call $|b_1/a_2|^2$ the backward transmission coefficient.

In the case of the practical circuits, we can assume the circuit parameters as follows:

$$S_{13} = S_{31} = S_{24} = S_{42} = jk$$
$$S_{12} = S_{21} = S_{43} = S_{34} = \sqrt{1-k^2}$$
$$\phi_f = \alpha_f + j\theta_f$$
$$\phi_b = \alpha_b + j\theta_b$$

where k is the coupling coefficient of the directional coupler.

The backward transmission coefficient is

$$P_b(\theta_b) = \left|\frac{b_1}{a_2}\right|^2 = \frac{(1-k^2) + e^{-2\alpha_b} - 2\sqrt{1-k^2}\,e^{-\alpha_b}\cos\theta_b}{1 + (1-k^2)e^{-2\alpha_b} - 2\sqrt{1-k^2}\,e^{-\alpha_b}\cos\theta_b}. \tag{5}$$

If the following condition is satisfied:

$$\theta_b = 2n\pi, \qquad n\text{: positive integer}$$

a resonance occurs in the resonator. At resonance the backward transmission coefficient becomes minimum as in a reaction type resonator:

$$P_b(2n\pi) = \left[\frac{\sqrt{1-k^2} - e^{-\alpha_b}}{1 - \sqrt{1-k^2}\,e^{-\alpha_b}}\right]^2. \tag{6}$$

Here, it should be noticed that the backward transmission coefficient vanishes when $\sqrt{1-k^2}$ is equal to $e^{-\alpha_b}$. It means that we can make the backward transmission vanish by adjusting the coupling coefficient k.

On the other hand, the forward transmission coefficient is

$$P_f(\theta_f) = \left|\frac{b_2}{a_1}\right|^2 = \frac{(1-k^2) + e^{-2\alpha_f} - 2\sqrt{1-k^2}\,e^{-\alpha_f}\cos\theta_f}{1 + (1-k^2)e^{-2\alpha_f} - 2\sqrt{1-k^2}\,e^{-\alpha_f}\cos\theta_f}. \tag{7}$$

When this circuit is used as an isolator, $P_f(\theta_f)$ and $P_b(\theta_b)$ correspond to the insertion loss and isolation, respectively. Furthermore, when the following condition is satisfied:

$$\theta_f = (2m-1)\pi, \qquad m\text{: positive integer}$$

the forward transmission coefficient becomes maximum.

Defining $Q_L = f_0/2(f_0 - f_1) = n\pi/\theta_1$, where f_1 and θ_1 are values of the half-power point, we have from (5)

$$P_b(\theta_1) = \tfrac{1}{2}[P_b((2n+1)\pi) + P_b(2n\pi)] \tag{8}$$

where $P_b((2n+1)\pi)$ and $P_b(2n\pi)$ correspond to the backward transmission coefficient at the "antiresonance" and "resonance", respectively. If θ_1 is small, we may replace $\cos\theta_1$ by $(1 - \theta_1^2/2)$ which yields

$$Q_L = \frac{n\pi}{\theta_1} \approx \frac{n\pi}{1 - \sqrt{1-k^2}\,e^{-\alpha_b}} \sqrt{\frac{1 + (1-k^2)e^{-2\alpha_b}}{2}} \left(\frac{\lambda_g}{\lambda_0}\right)^2. \tag{9}$$

Furthermore, if α_b is small, the loaded Q at $\sqrt{1-k^2} = e^{-\alpha_b}$ is about one half of the unloaded Q which is defined by $n\pi/\alpha_b \cdot (\lambda_g/\lambda_0)^2$. This just corresponds to the critical coupling condition in a one-port cavity resonator circuit. The circuit which satisfies the critical coupling condition becomes the isolator with perfect isolation.

III. Magnetized Ferrite Pillbox as the Nonreciprocal Traveling-Wave Resonator

A nonreciprocal traveling-wave circuit is realized with a magnetized ferrite pillbox resonator distributionally coupled to a dielectric waveguide, as shown in Fig. 2.

As the pillbox is a closed-loop structure in itself, the wave coupled through the coupling region once travels along the θ-direction and returns to the coupling region again. The difficulty in solving the coupling problem on this structure is caused by this feedback mechanism.

Consider the model as shown in Fig. 3, where axis u is a hypothetical axis. Circular disks, which are cut as shown in Fig. 3(a), are connected to each other in a spiral-like manner in the hypothetical space as shown in Fig. 3(b), where it is assumed that the boundary conditions on the interface between the spiral region and the air region are the same as those of the corresponding pillbox in real space. The cut in Fig. 3(a) and each disk of the spiral model in Fig. 3(b) can be regarded as a branch cut and a Riemann surface, respectively. In addition, this spiral model is regarded as a waveguide like the ordinary image lines.

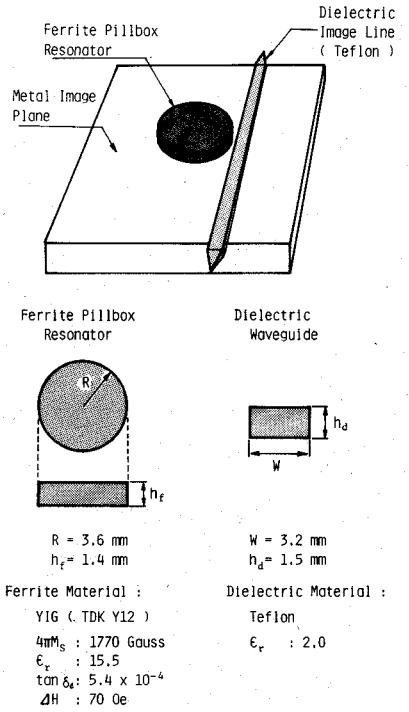

Fig. 2. Experimental image-line isolator, giving performance data of Fig. 11 and Table II.

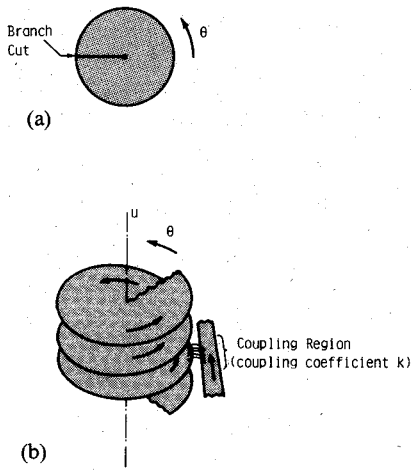

Fig. 3. Hypothetical spiral waveguide for the estimation of the coupling coefficient.

The coupled wave through the coupling region can travel in this spiral waveguide toward the positive θ-direction. In this waveguide, we can exclude the physical requirement of the pillbox where the field must be single-valued at any point in the θ-direction. Therefore, nonintegral values can be assigned to ν which is the order of Bessel function $J_\nu(\eta r)$ that expresses the field E_y in the spiral waveguide.

The coupling coefficient between the spiral waveguide and a straight waveguide corresponds to the coupling coefficient k of the directional coupler in the previous section. And now, we can evaluate the coupling coefficient all over the frequency range because there is no restriction in ν. The circuit responses of the pillbox circuit in Fig. 2, P_b and Q_L, are regarded as the total circuit response of the closed-loop structure consisting of the spiral waveguide

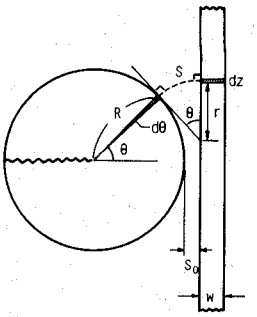

Fig. 4. Coupling structure consisting of a spiral waveguide and a straight waveguide.

including the coupling region and can be obtained from (5) and (9). When ν becomes integer, a resonance occurs in the corresponding pillbox because the traveling waves are combined in phase as in the case of the ring resonators [6]–[8].

A. Propagation Constants

Consider the coupling structure shown in Fig. 4 in order that we may estimate the coupling coefficient. We assume that the wavefronts are normal to the propagation direction and these fronts form cylindrical planes between the spiral waveguide and the straight dielectric waveguide. Spacing S between the incremental coupling lengths of the two waveguides corresponds to the length of the circular arc S and is given by the following equations [10], [11]:

$$S = r\theta \tag{10}$$

$$r = \frac{S_0 + R(1-\cos\theta)}{\sin\theta} \tag{11}$$

where S_0 is the smallest spacing and θ is the angle subtended by the arc S.

First, we must know the propagation modes and their propagation constants in the three structures, i.e., the spiral waveguide, the straight dielectric waveguide, and the coupling structure which consists of both of them.

Here, we reduce the three-dimensional model into the slab model by using the effective dielectric constant method [12]. The relative dielectric constant ϵ_r of the material is replaced by the effective dielectric constant which is given as

$$\epsilon_{re} = \epsilon_r - (\beta_y/k_0)^2. \tag{12}$$

The propagation constant in the z-direction is, in turn, obtained by

$$\beta_z^2 = \epsilon_{re}k_0^2 - \beta_x^2. \tag{13}$$

The eigenvalue equation for the straight dielectric waveguide is

$$\eta_3 \sin\eta_3 w - \eta_0 \cos\eta_3 w = 0 \tag{14}$$

where

$$\beta_z^2 = k_0^2 + \eta_0^2 = \epsilon_{re3}k_0^2 - \eta_3^2.$$

Also, the eigenvalue equation for the spiral waveguide is

$$\{\eta_0 R - \nu\}J_\nu(\eta_1 R) + \eta_1 R J_{\nu-1}(\eta_1 R) = 0 \tag{15}$$

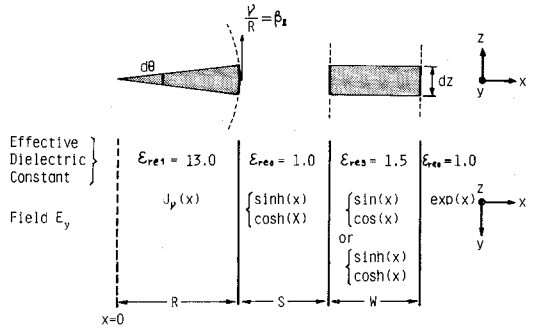

Fig. 5. Structure for analyzing x variations using concept of effective dielectric constants. $\epsilon_{re1} = 13.0$ was determined by considering the small gap between a ferrite pillbox and a metal image plane because of using an adhesive tape.

where

$$\beta_z^2 = \left(\frac{\nu}{R}\right)^2 = k_0^2 + \eta_0^2 \qquad \text{and} \qquad \eta_1^2 = \epsilon_{re1} k_0^2.$$

On the other hand, the eigenvalue equation for the coupling structure as shown in Fig. 5 is

$$\begin{aligned}&\eta_3\{\eta_0\cos(\eta_3 w) - \eta_3\sin(\eta_3 w)\}\\ &\cdot\{\eta_0 J_\nu(\eta_1 R) + \eta_1 J_\nu'(\eta_1 R)\cdot\tanh(\eta_0 S)\}\\ &+\eta_0\{\eta_0\sin(\eta_3 w) + \eta_3\cos(\eta_3 w)\}\\ &\cdot\{\eta_0 J_\nu(\eta_1 R)\cdot\tanh(\eta_0 S) + \eta_1 J_\nu'(\eta_1 R)\} = 0 \end{aligned} \quad (16)$$

where

$$\tilde{\beta}_z^2 = \left(\frac{\nu}{R}\right)^2 = k_0^2 + \eta_0^2 = \epsilon_{re3} k_0^2 - \eta_3^2$$

and

$$\eta_1^2 = \epsilon_{re1} k_0^2.$$

Here, when the following relation is satisfied:

$$\epsilon_{re3} k_0^2 < \left(\frac{\nu}{R}\right)^2$$

we must change η_3 into $j\eta_3$.

In the preceding, η_0, η_1, and η_3 are the x-direction propagation constants (or the phase constants) in the air region, the spiral waveguide, and the straight dielectric waveguide, respectively. And, of course, ν takes a nonintegral value.

B. Theoretical and Experimental Estimations of the Coupling Coefficient

We are interested in only one mode in the spiral waveguide because we consider the circuit response around a resonance by which one mode is selected. Therefore, we can estimate the coupling coefficient k by the perturbation method as follows [13]:

$$|S_{21}| = \sqrt{1-|k|^2} = \sqrt{1-(\xi A_0 \sin(KL))^2} \quad (17)$$

$$|S_{31}| = |k| = \xi A_0 |\sin(KL)| \quad (18)$$

where

$$KL = 2\int_0^{\pi/2} \frac{\tilde{\beta}_i(\theta) - \tilde{\beta}_1(\theta)}{2} R\, d\theta \quad (19)$$

and

$$A_0 = \sqrt{1 - \left(\frac{\beta_i - \beta_1}{\tilde{\beta}_i(0) - \tilde{\beta}_1(0)}\right)^2} \quad (20)$$

where

- A_0 maximum coupling coefficient,
- ξ correction factor (≈ 1.0),
- β_1 phase constant in the straight dielectric waveguide,
- β_i phase constant of the ith mode in the spiral waveguide ($= \nu/R$),
- $\tilde{\beta}_1, \tilde{\beta}_i$ phase constants in the coupling structure which consists of the straight waveguide and the spiral waveguide,

and the modes in the straight dielectric waveguide are restricted to the dominant one. Also, β_j and $\tilde{\beta}_j$ are related as follows:

$$\tilde{\beta}_j = \beta_j + \Delta\beta_j \qquad (j = 1,2,\cdots,n)$$

where $\Delta\beta_j$ is assumed to be small and $\tilde{\beta}_j$ is asymptotic to β_j as the spacing S approaches to infinity.

The coupling coefficient k cannot be measured directly because the pillbox resonator is a closed-loop structure in itself. Therefore, the coupling coefficient must be determined through the measured circuit responses, i.e., P_b and Q_L. Here, by considering (6) and (9), we define an evaluation function F for minimizing the difference between theoretical and measured values as follows:

$$\begin{aligned}F(A,T) = \sum_{i=1}^{n} \Bigg\{ &a_i\left[P_{bi} - \left(\frac{T_i - A}{1 - T_i A}\right)^2\right]^2\\ &+ b_i\left[Q_{Li} - \frac{n\pi}{1 - T_i A}\sqrt{\frac{1 + T_i^2 A^2}{2}}\cdot\left(\frac{\lambda_g}{\lambda_0}\right)^2\right]^2\Bigg\} \end{aligned} \quad (21)$$

where

$$T_i = \sqrt{1 - k_i^2}$$

$$A = e^{-\alpha_b}$$

and

- k_i coupling coefficient,
- P_{bi} measured P_b at resonance,
- Q_{Li} measured Q_L,
- n number of measured points as a function of the spacing, and
- a_i, b_i weighting factors,

and the weighting factors a_i and b_i must be introduced when there are great differences in the order of magnitude between P_{b_i} and Q_{L_i}. The computer optimization is performed by Powell's minimizing method [14], where we can find out the optimum values of $e^{-\alpha_b}$ and k_i which minimize the evaluation function F.

Fig. 6 shows the frequency responses of the measured P_b at several spacings. The computer optimization yielded $e^{-\alpha_b}$ and k_i from the measured P_b and Q_L, and they are

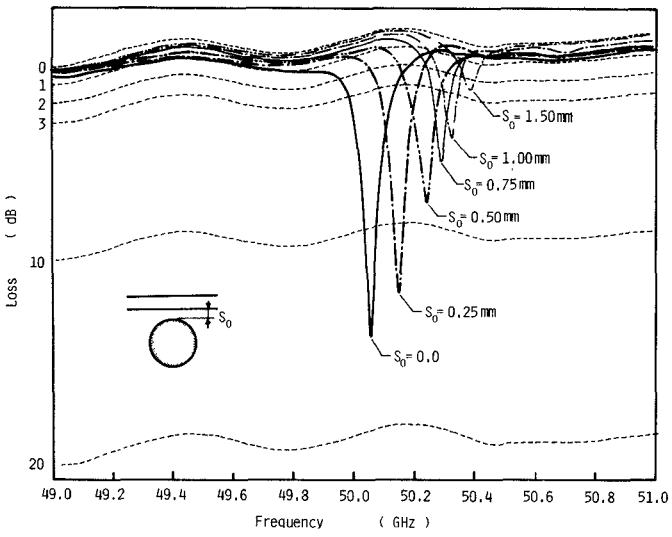

Fig. 6. Frequency responses of the measured P_b at several spacings for the isolator of Fig. 2.

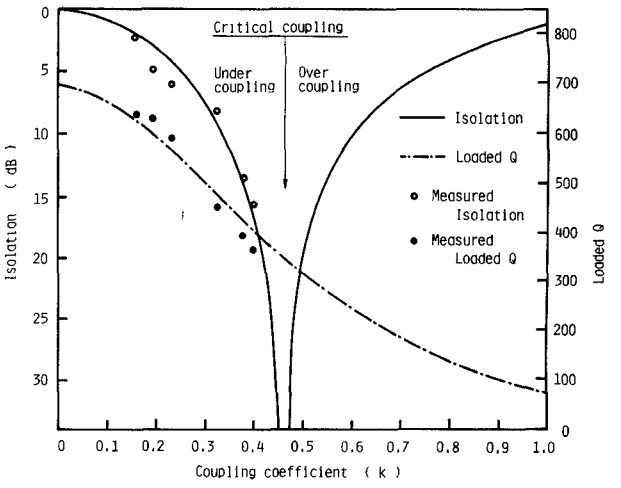

Fig. 7. Theoretical and experimental circuit responses for the isolator of Fig. 2 as a function of the coupling coefficient.

plotted in Fig. 7 with the theoretical circuit responses, where $e^{-\alpha_b}$ was assumed to be 0.889. From this figure, we knew the experimental circuit was in the under coupling region at all the spacings.

The theoretical and experimental coupling coefficients are shown in Fig. 8 as a function of the spacing. Although there are three modes in the experimental circuit, we can find out the coupled mode by the difference of a pair of measured resonant frequencies as discussed in the next section, where we can find that the coupled mode is mode 2. The correction factor ξ is determined experimentally. The theoretical values of the coupling coefficient are shown to be in relatively good agreement with the experimental values for $\xi = 0.9$.

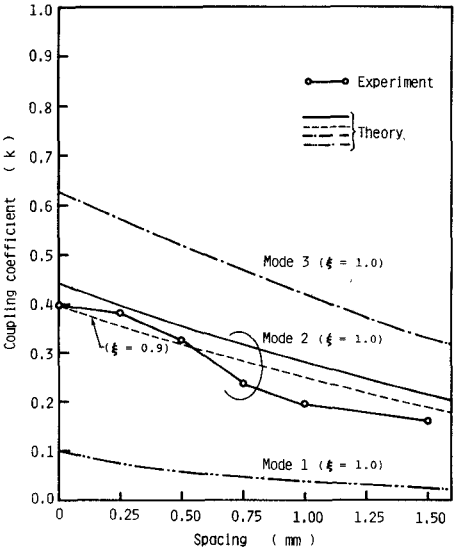

Fig. 8. Theoretical and experimental coupling coefficients for the isolator of Fig. 2 as a function of spacing S_0.

C. Nonreciprocity of Ferrite Pillbox Resonators

When the external dc magnetic field is applied to a ferrite pillbox resonator, a pair of degenerate modes split into clockwise and counter-clockwise modes, as shown in Fig. 9. If κ/μ is small, the difference of a pair of resonant frequencies is determined by the following equations [3]:

$$f_w \approx \left(\frac{C_0}{2\pi R}\right)^2 \cdot \frac{2n x_{n,j}^2}{\epsilon_{re1}\mu f_0\left(x_{n,j}^2 - n^2\right)} \cdot \frac{\kappa}{\mu} \tag{22}$$

where

$$x_{n,j} \approx \frac{2\pi f_0 \sqrt{\epsilon_{re1}\mu_{eff}}}{C_0} \cdot R \tag{23}$$

where

C_0 speed of light in free space,
f_0 resonant frequency without dc magnetization,
n order of the resonant mode,
$x_{n,j}$ jth solution of the nth order equation $J_n'(x) = 0$,

and μ and κ are diagonal and off-diagonal coefficients of the permeability tensor for magnetization in the y-direction. The effective specific permeability μ_{eff} is given by

$$\mu_{eff} = \left(\mu^2 - \kappa^2\right)/\mu. \tag{24}$$

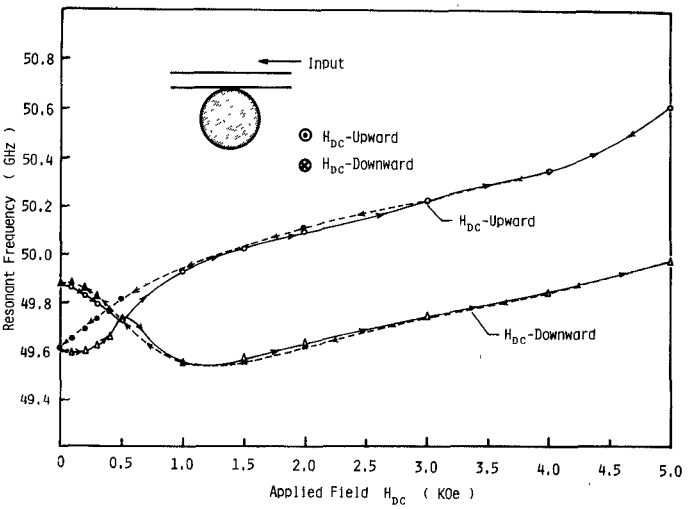

Fig. 9. Measured resonant frequencies for the ferrite pillbox of Fig. 2 as a function of dc magnetic field.

TABLE I
RESONANT MODES IN THE FERRITE PILLBOX RESONATOR OF FIG. 2 AROUND 50 GHz

	$x_{n,j}$	f_W (GHz)
$TM_{11,1,\delta}$ (Mode 1)	12.8	2.25
$TM_{7,2,\delta}$ (Mode 2)	12.9	0.54
$TM_{4,3,\delta}$ (Mode 3)	12.7	0.24

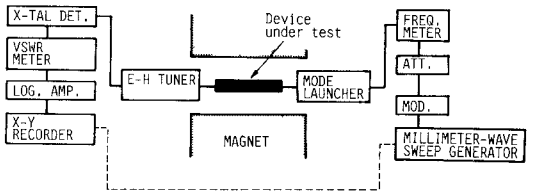

Fig. 10. Block diagram for measurement.

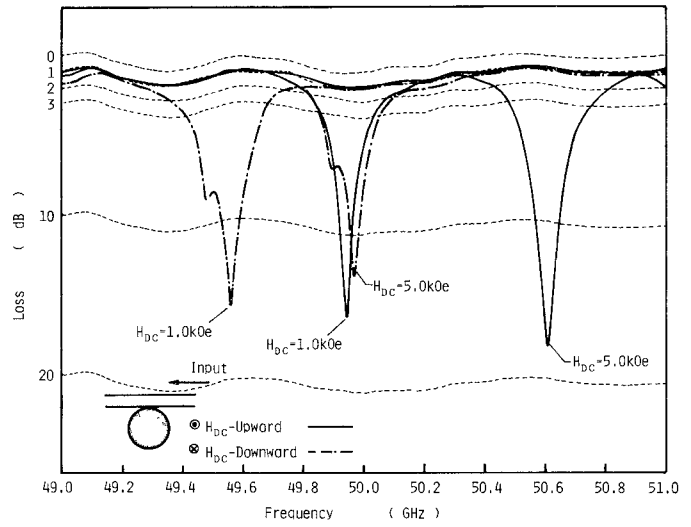

Fig. 11. Measured characteristics of the isolator with one ferrite pillbox of Fig. 2, where spacing $S_0 \approx 0$.

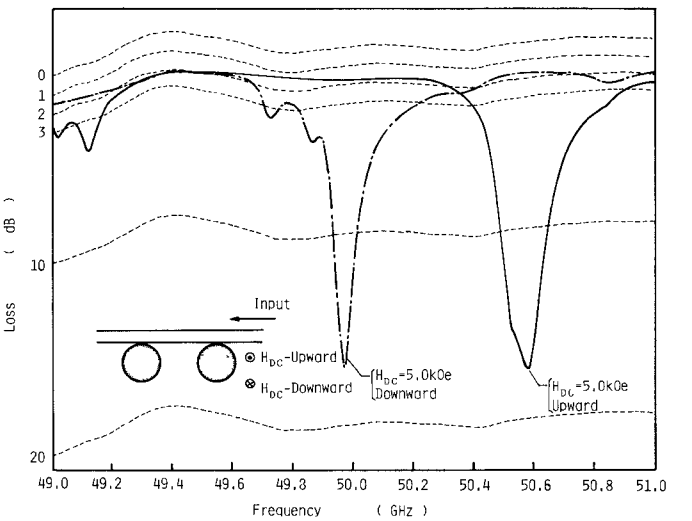

Fig. 12. Measured characteristics of the isolator with two ferrite pillboxes, where spacing $S_0 \approx 0$.

TABLE II
CHARACTERISTICS OF THE IMAGE-LINE ISOLATORS

	One Pillbox Type	Two Pillbox Type
Center Frequency	50.61 GHz	50.58 GHz
Isolation	18 dB	17 dB
Insertion Loss	1.0 dB	1.8 dB
15dB Bandwidth	50 MHz	100 MHz
Biasing Field	5000 Oe	5000 Oe
Ferrite Pillbox	YIG (TDK Y12) radius = 3.6mm thickness = 1.4mm	YIG (TDK Y12) radius ≈ 3.6mm thickness = 1.4mm

In the estimation, by assuming a cylindrical surface containing the circumference of the pillbox resonator as a magnetic wall, there are three resonant modes in the pillbox around the 50 GHz for $R = 3.6$ mm, $\epsilon_r = 15.5$, and $\mu \approx 1.0$. From Table I and Fig. 9, it can be determined that the resonant mode in the experimental pillbox was $TM_{7,2,\delta}$ because the difference of a pair of resonant frequencies was about 0.5 GHz in the case of saturation.

IV. ISOLATOR FOR MILLIMETER-WAVE INTEGRATED CIRCUITS

The structure of the image-line isolator is quite simple, as shown in Fig. 2. This consists of a ferrite pillbox and a teflon image line.

Fig. 10 shows the block diagram of the experimental setup. The EH tuner was adjusted to obtain the maximum output power and to reduce the reflection at the output port. The 0-dB reference was determined by removing the ferrite pillbox resonator. The insertion loss and isolation were measured by changing the direction of the dc magnetic field instead of changing the input port.

Fig. 11 shows the characteristics of the isolator with one ferrite pillbox. Although the isolation is high, it is not infinite. That is the reason why the critical coupling condition could not be satisfied in our experimental circuit in spite of $S_0 = 0$ (see Fig. 7). To get the critical coupling, we need the ferrite pillbox whose loss is lower than the present one. The bandwidth or isolation can be improved if a cascade connection of resonators is employed. Fig. 12 shows the characteristics of the isolator with two ferrite pillboxes. In practice, however, the improvement by the cascade connection has been achieved at the expense of the insertion loss. A summary of the isolator performance achieved is presented in Table II.

V. CONCLUSION

The nonreciprocal traveling-wave resonator critically coupled to a waveguide has many interesting features. As one of its applications, the image-line isolator using a magnetized ferrite pillbox resonator was investigated experimentally and theoretically. Although the frequency bandwidth of this isolator was very narrow, because of

using the resonant phenomenon, it has many attractive features: 1) the isolation is very high; 2) the insertion loss is low; and 3) the operation frequency can be swept by changing the applied magnetic field.

The theoretical and experimental estimations of the coupling coefficient between a pillbox resonator and a straight dielectric waveguide were also investigated. This analysis has shown much better agreement with experimental result in the case of the dominant mode resonator.

ACKNOWLEDGMENT

The authors wish to thank the Yokosuka Electrical Communication Laboratory, Nippon Telegraph and Telephone Public Corporation, Yokosuka, Japan, for supplying several millimeter-wave components. Also, the authors would like to express their thanks to the reviewers for helpful advices which have improved the readability of this paper.

REFERENCES

[1] R. M. Knox, "Dielectric waveguide microwave integrated circuits—An overview," *IEEE Trans. Microwave Theory Tech.*, vol. MTT-24, pp. 806–814, Nov. 1976.

[2] V. P. Nanda, "A new form of ferrite device for millimeter-wave integrated circuits," *IEEE Trans. Microwave Theory Tech.*, vol. MTT-24, pp. 876–879, Nov. 1976.

[3] M. Muraguchi and Y. Naito, "Nonreciprocal device in open-boundary structures for millimeter-wave integrated circuits," *IECE Jap. Trans. B.*, vol. 64-B, pp. 604–611, July 1981.

[4] I. Awai and T. Itoh, "Coupled-mode theory analysis of distributed nonreciprocal structures," *IEEE Trans. Microwave Theory Tech.*, vol. MTT-29, pp. 1077–1087, Oct. 1981.

[5] K. Araki and T. Itoh, "Analysis of periodic ferrite slab waveguides by means of improved perturbation method," *IEEE Trans. Microwave Theory Tech.*, vol. MTT-29, pp. 911–916, Sept. 1981.

[6] K. Tomiyasu, "Attenuation in a resonant ring circuit," *IEEE Trans. Microwave Theory Tech.*, vol. MTT-8, pp. 253–254, Mar. 1960.

[7] G. L. Matthaei *et al.*, *Microwave Filters, Impedance-Matching Networks, and Coupling Structures.* New York: McGraw-Hill, 1964, ch. 14.

[8] F. J. Tisher, "Resonant properties of nonreciprocal ring circuits," *IRE Trans. Microwave Theory Tech.*, vol. MTT-6, pp. 66–71, Jan. 1958.

[9] E.-G. Neumann and H.-D. Rudolph, "Radiation from bends in dielectric rod transmission lines," *IEEE Trans. Microwave Theory Tech.*, vol. MTT-23, pp. 142–149, Jan. 1975.

[10] T. Itanami and S. Shindo, "Channel dropping filter for millimeter-wave integrated circuits," *IEEE Trans. Microwave Theory Tech.*, vol. MTT-26, pp. 759–764, Oct. 1978.

[11] T. Trinh and R. Mittra, "Coupling characteristics of planar dielectric waveguides of rectangular cross section," *IEEE Trans. Microwave Theory Tech.*, vol. MTT-29, pp. 875–880, Sept. 1981.

[12] T. Itoh, "Inverted strip dielectric waveguide for millimeter-wave integrated circuits," *IEEE Trans. Microwave Theory Tech.*, vol. MTT-24, pp. 821–876, Nov. 1976.

[13] K. Kurokawa, *An Introduction to the Theory of Microwave Circuits.* New York: Academic Press, 1969, ch. 6.

[14] M. J. D. Powell, "A method for minimizing a sum of squares of nonlinear functions without calculating derivatives," *Comput. J.*, vol. 7, pp. 303–307, 1965.

Masahiro Muraguchi (S'81) was born in Kanazawa, Japan, on May 23, 1955. He received the B.S. degree in electrical engineering from the Nagoya Institute of Technology, Nagoya, Japan, in 1978, and the M.S. degree in physical electronics engineering from the Tokyo Institute of Technology, Tokyo, Japan, in 1980. He is currently studying toward the Ph.D. degree at the Tokyo Institute of Technology, where he has been working on the millimeter-wave integrated circuits and components.

Mr. Muraguchi is a member of the Institute of Electronics and Communication Engineers of Japan.

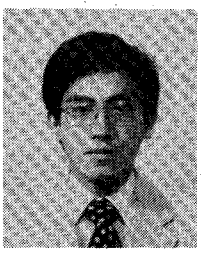

Kiyomichi Araki was born in Nagasaki, Japan, on January 7, 1949. He received the B.S. degree in electrical engineering from Saitama University, Urawa, Japan, in 1971, and the M.S. and Ph.D. degrees in physical electronics engineering, both from the Tokyo Institute of Technology, Tokyo, Japan, in 1973 and 1978, respectively.

From 1978 to the present he has been a Research Associate at Tokyo Institute of Technology. From September 1979 to August 1980 he was a Post Doctoral Fellow at the University of Texas, Austin, where he was engaged in the design and development of millimeter wave devices.

Dr. Araki is a member of IECE of Japan, from which he received a Young Engineer Award in 1979.

Yoshiyuki Naito (M'70–SM'74) was born in Oita, Japan, on November 22, 1936. He received the B.S. degree in electrical engineering and the D.Eng. degree, from the Tokyo Institute of Technology, Tokyo, Japan, in 1959 and 1964, respectively.

Since 1964 he has been with the Tokyo Institute of Technology. From September 1965 to October 1966 he was a Postdoctoral Fellow at the Polytechnic Institute of Brooklyn, Brooklyn, NY. Currently, he is a Professor with the Faculty of Engineering. His research has chiefly been concerned with microwave circuit elements and properties and applications of magnetic material and antennas.

Dr. Naito received an Inada Award in 1961 and a Treatise Award in 1966 from the Institute of Electronics and Communication Engineers of Japan. He is a member of the Institute of Electronics and Communication Engineers of Japan.